Ministry of Science, Research and Technology
Institute for Color Science and Technology

Ultrafine Titanium-dioxide (Rutile) Based Nano-crystalline Dispersions as a Pigment for Waterborne Coatings

P. Shah[*1], N. Agrawal[2], N. Reddy Ravuru[1], S. Patel[1]

[1.] Department of Chemical Engineering, Institute of Technology, Nirma University, Ahmedabad, PIN: 382481, Gujarat, India

[2.] Chemical Engineering Department, Pandit Deendayal Energy University, Gandhinagar, PIN: 382007, Gujarat, India

ABSTRACT

*T*he present study involves a novel approach in manufacturing nano-crystalline dispersions of titanium dioxide, a widely used pigment in the paints and coatings market. These dispersions are developed to provide certain benefits over conventional titanium dioxide powder to improve the coating parameters such as adhesion promotion, hiding, tinting strength, dispersion, and reduced dosage. Dispersions are synthesized using bead mill and high-speed disperser in a unique multi-stage process, thereby developing a scalable technology for industrial synthesis. Characterization of these dispersions, namely XRD, particle size analysis, and FE-SEM, confirmed the presence of nano-crystalline titanium dioxide particles. Moreover, analysis of process variables was also conducted by studying the effect of grinding time on particle-size reduction. Rheological analysis was performed for water and styrene-acrylic copolymer emulsion systems. It was developed a dataset of viscosities. Results of this study can be assessed to create scalable technology for the synthesis of nano-crystalline dispersions, which can be used as a pigment in multipurpose waterborne coating systems. Prog. Color Colorants Coat. 15 (2022), 305-318© Institute for Color Science and Technology.*

1. Introduction

Titanium dioxide is one of the most used pigments globally, with its global market estimated at over a whopping 16.98 billion USD (2020). The potential growth approximated at the CAGR of 8.3 % over the next seven years to 26.84 billion by the year 2028 [1]. It is used as a primary white inorganic pigment for various applications, including paints & coatings, textile, cosmetics, pulp & paper, food, and ceramic industries. It has wide adaption across the range of industries due to many factors: first and foremost, widespread use of white color in several applications, secondary due to its dispersion into the range of chemicals, and lastly due to its photostability along with good whiteness and brightness [2]. Paints and coatings are the major consumer sector of this pigment, holding about 55 %. The widely used grade in the coatings sector is the chloride processed rutile-grade titanium dioxide due to its superior pigment properties, especially whiteness, over its anatase counterpart. At present, the physical form of the pigment essentially remains to be the solid white powder, which is dispersed into the system during the formulation process [3].

Present work describes the synthesis and application of the ultrafine aqueous dispersions of the titanium dioxide as a pigment dispersion into the range of waterborne coatings. Ultrafine aqueous titanium-dioxide

*Corresponding author: 17bch032@nirmauni.ac.in

dispersions are made using chloride processed titanium dioxide, water, and a range of additives to impart and improve paint properties such as wetting, adhesion promotion, dispersion, tinting strength, and gloss [4]. Wetting accounts for solid-liquid contact at the substrate interface due to intermolecular interactions. Flow and leveling agents are dispersant polymers that allow high mineral incorporation in the system and stabilize it through an electro-steric repulsion mechanism, which ultimately leads to adhesion promotion since these surfactants create a molecular bridge between the particles. Tinting strength. The motive of developing high solids pigment dispersion is to improve its properties over conventional commercially available pigment powders by using ultrafine grinding, improving properties with the help of additives, easing the handling, storage, and incorporation of the pigment dispersion into the coatings [5].

2. Experimental

2.1. Materials

The materials used in the synthesis are all *industrial-grade chemicals* to demonstrate the scalability of this technology. The titanium dioxide used to synthesize pigment dispersion is chloride processed rutile-BLR-895 grade. Rheology modifier Hydroxyethyl Cellulose along with the number of additives; flow and leveling agent (Acrylic Polymer CE-SD), wetting agent (SP-100 Additive), in-can preservative, pearl pigment(icy-white), photo-bleaching agent, and structuring agent (Additive PA-63) and pigment extender calcined kaolin were sincerely provided by PK Enterprise (Ahmedabad, India). Distilled water was used as an aqueous media for preparing the pigment dispersion. Liquor ammonia with a specific gravity of 0.9 and 24-25 % concentration was used to neutralize amine.

2.2. Synthesis of pigment dispersions

The synthesis process of the ultrafine titanium-dioxide dispersions was designed into a 3-step formulation. It led to obtaining ultrafine particle size and distribution of the coating. The first stage involves pre-mixing the titanium dioxide, base thickener, and other surfactants. The next stage is the grinding stage, which brings down the particle size of the pigment, is carried out in the bead mill. The final let-down stage is carried out in a high-speed disperser in which additives are added into the system to impart other paint-enhancing

properties to the dispersion [6].

2.2.1. Pre-mixing stage

The pre-mixing stage involves preparing the base jelly of the dispersions using a rheology modifier. Twenty-five parts of water and 00.40-00.60 % w/wt rheology modifier (different compositions of HEC in different batches) along with 0.05% of the neutralizing amine (liquor ammonia) were taken to prepare the base jelly to incorporate desired viscosity into the final pigment dispersion with a motive to improve the rheological properties of the waterborne coatings [7]. The process was carried out in a high-speed stirrer at 500 RPM for 15 minutes to allow the rheology modifier to build up the viscosity ultimately.

2.2.2. Grinding stage

The grinding stage was carried out in the batch-process bead mill. It was selected for particle grinding to bring particle size to the sub-micron range to improve the dispersion properties. The pre-mixed solution was directly subjected to milling to bring down the particle size of the pigment. The samples were subjected to a 2-stepped grinding process to obtain ultrafine dispersions, in which first stage was carried out for 4 hours and the second stage for 3 hours at 960 RPM in the mill using 4-5 mm glass beads as grinding media [8]. The process was designed after conducting the particle size and distribution analysis of titanium dioxide powder to bring down its particle size and narrow its size distribution (polydispersity) to achieve nano-crystals of the material. Samples were taken from the mill after a range of intervals to study the effect of grinding time on particle size dispersion. The material was discharged from the bead mill post grinding into the high-speed disperser [9].

2.2.3. Let-down stage

The let-down stage was processed in the high-speed disperser equipped with the variable frequency drive. This stage was carried out to ensure the uniform dispersion of the post-addition chemicals. The discharged material from the bead mill was incorporated into the disperser and subjected to the high-shear (range 1200-1800 rpm). Non-grinding stage chemicals were added in this stage for homogeneous dispersion into the paste [10]. Icy white pearl pigment and photo-bleaching agent were added after the system was stirred for 15 minutes. The structuring agent was diluted in the make-

up water, added into the batch, and stirred for 30 minutes to minimize agglomeration. The system was gradually brought to lower rpm, stirred for about 5 minutes before stopping to reduce the generation of the foams [11].

Different batches were formulated with variations in the compositions of hydroxyethyl cellulose, titanium dioxide powder pigment, and its partial replacement using functional filler-calcined kaolin. These formulations were developed different pigment dispersions to compare their pigment and other physiochemical properties. Purpose of making changes in these chemicals for the synthesis of different dispersions:

Hydroxyethylcellulose imparts viscosity and flow properties to them, so different compositions were taken to develop dispersions that are suitable for a range of waterborne coatings; Titanium dioxide, the primary pigment, was partially replaced with calcined kaolin in some formulations to develop economical dispersions [12]. The synthesized pigment dispersions were also subjected to various characterization techniques to study their properties. The table below contains designation assigned to different pigment dispersions that have been synthesized (Figure 1).
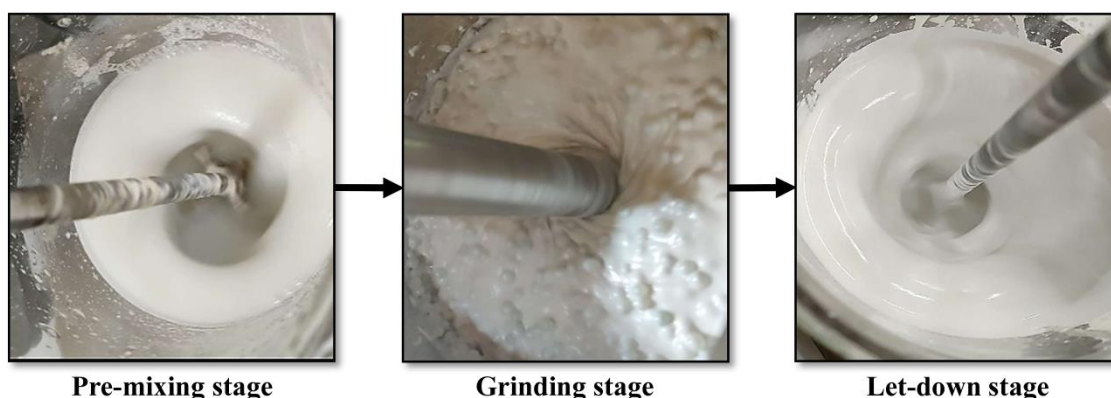

Figure 1: Synthesis stages of PD-T70-Th5 pigment dispersion (top-view images).

Table 1: Designation of pigment dispersions on the composition basis.

Sr. No.	Designation	Composition			
		TiO_2 (% w/w)	HEC (% w/w)	Filler	
				Material	Composition
1	PD-T70-Th4	70	0.4	-	-
2	PD-T70-Th5	70	0.5	-	-
3	PD-T70-Th6	70	0.6	-	-
4	PD-T50-K20-Th4	50	0.4	Calcined Kaolin	20 % (w/w)
5	PD-T50-K20-Th5	50	0.5	Calcined Kaolin	20 % (w/w)
6	PD-T50-K20-Th6	50	0.6	Calcined Kaolin	20 % (w/w)

2.3. Characterization of pigment dispersions

The synthesized pigment dispersions were characterized to understand their morphology and structure. Particle-size analysis and distribution were performed by Horiba SZ-100 Particle Size Analyzer. Fourier-transformed Infrared Spectroscopy performed bond detections by Jasco FT/IR-6100typeA spectrometer, and surface morphology was investigated by field emission scanning electron microscopy (FE-SEM) using JSM-7600F Schottky field emission scanning electron microscope, as described previously [13]. Moreover, crystallographic analysis was carried out using X-ray diffraction using Bruker D8 advance diffractometer. The measurement of physicochemical properties was also carried out as per ASTM standards.

2.4. Analysis of process variables

In-depth research analysis of the crucial parameters and their impact upon the concerned product properties was conducted to obtain a dataset that states the output for different processing conditions to give an idea to tailor the product as per desired specifications. Two main analyses were conducted, the first of which is the effect of grinding time on the average particle size of the pigment and the second being the rheological parameters associated with the pigment [14]. Particle size (d_{50}) as a function of grinding time was studied to understand the nature of the size reduction process in the milling process. Moreover, in-depth rheological analysis was conducted by measuring kinematic viscosities. Different proportions of the dispersions and the water with styrene-acrylic copolymer emulsion, which forms the base of waterborne coatings, were used to measure kinematic viscosities [15].

3. Results and Discussion

3.1. Characterization of the pigment dispersions

3.1.1. Particle size analysis and distribution

The dispersions were subjected to particle size analysis utilizing the Horiba SZ-100 PSA instrument (size range of 0.3 nm to 8.0 μm). The research was carried out at 25 °C with a scattering angle set to 90°. Analysis was carried out in standard distribution form with dispersity set to monodisperse. Titanium dioxide powder pigment and synthesized dispersions were subjected to PSA to evaluate size reduction, which is crucial in determining pigment properties. Powder and pigment dispersions were diluted in the distilled water to the concentration of 10 ppm. The processing variables and results have been shown in the Table 2, and particle size distribution curves are shown in Figure 2.

As measured by the device for the sample solutions, the sample viscosity of powder, PD-T70-Th5, and PD-T50-K20-Th5 was 0.897, 0.899, and 0.895 mPa.s, respectively. Table 2 lists important particle size data and calculations related to the measurement and analysis.

Table 2: PSA histogram & calculation results for pigment powder & dispersion.

Sr. No	Designation	Count Rate (kCPS)	Particle Size Distribution (nm)			Cumulant Operations	
			< 10 %	< 50 %	< 90 %	Z-Average (nm)	Polydispersity (PI)
1	Ti_Powder	402	824.3	1121.3	1584.5	2531.8	0.614
2	PD-T70-Th5	85	32.8	49.9	79.5	45.9	0.285
3	PD-T50-K20-Th5	111	136.9	183.4	250.7	196.5	0.355
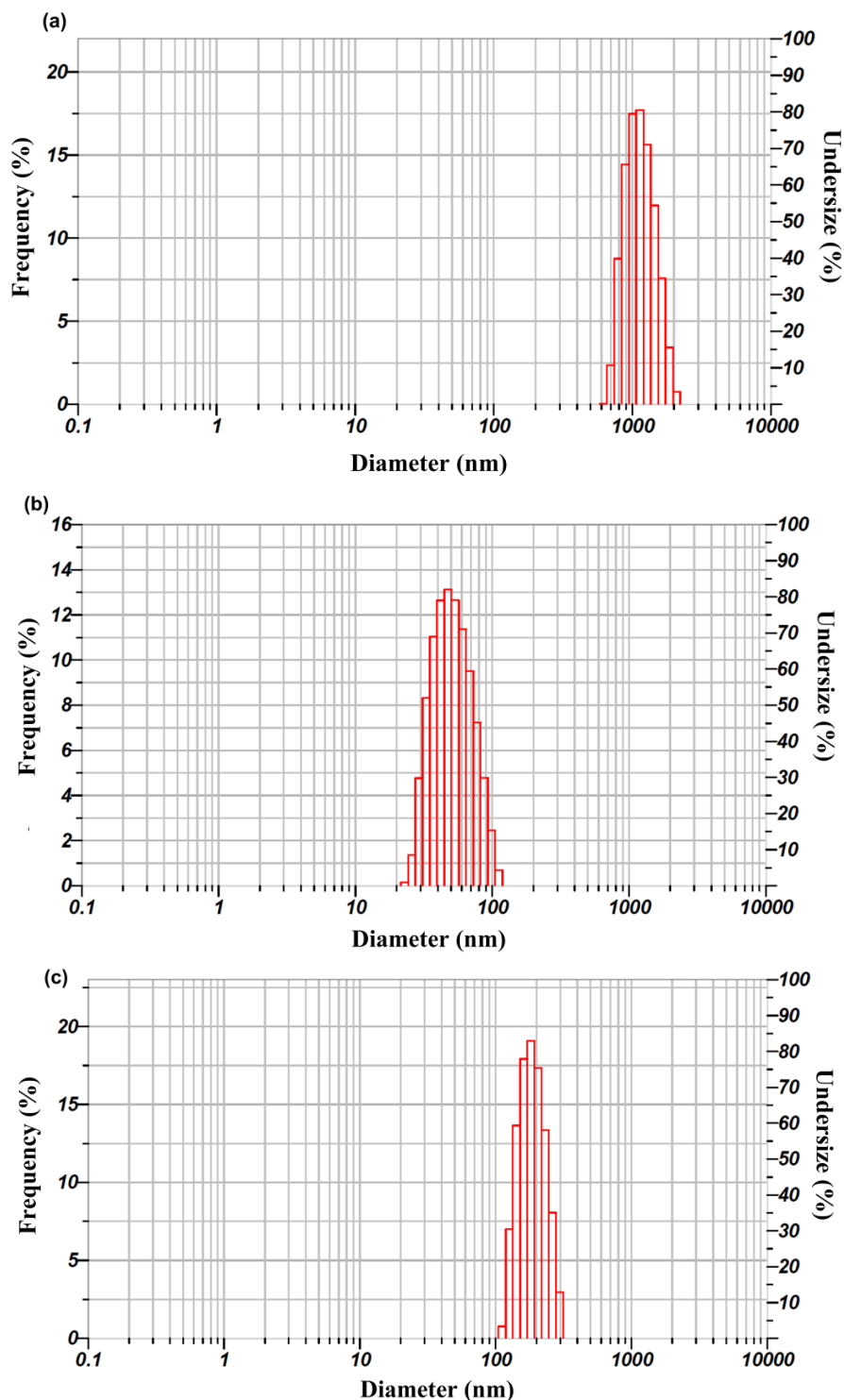
Figure 2: PSA histogram of titanium dioxide powder (a), PD-T70-Th5 (b) and PD-T50-K20-Th5 (c).

The pigment dispersion PD-T70-Th5 and PD-T50-K20-Th5 were found to undergo the size-reduction of approximately 22.50 and 6.14 times, respectively, in the particle-size distribution (<50 %). The reduction in polydispersity index was also found in the pigment dispersion, which indicates the narrow particle size distribution at 0.285 and 0.355 for PD-T70-Th5 and PD-T50-K20-Th5 dispersions, respectively. It is the essential meaning factor for the range of particle sizes in samples as it governs functional properties such as whiteness, dispersion, hiding and coverage [16]. Moreover, the z-average cumulative operation, as

carried out by the instrument's software, provides close z-average and d_{50} particle size for PD-T70-Th5 nano-dispersions, which relates to their high stability against aggregation, which they can be considered as 'weakly interacting particles. The interaction factor for PD-T50-K20-Th5 is relatively higher, yet they are quite stable against the higher agglomeration of nanoparticles. The wide difference in these values in the case of titanium dioxide powder is associated with the tendency of its particles to agglomerate and form clusters since they possess 'highly interacting particles' [17].

3.1.2. Fourier transform infra-red spectroscopy (FT-IR)

The FT-IR spectra analysis was carried out using Jasco 6100 type-A spectrometer to detect and evaluate bonds present in the pigment dispersions. The investigation was carried out for the wavenumber range from 400-6000 cm^{-1}. The resolution was kept to 16 cm^{-1} and scanning speed at two mm/s with a filter of 10,000 Hz. Titanium dioxide powder, dispersions PD-T70-Th5 and PD-T50-K20-Th5 were subjected to FT-IR to identify and compare functional groups present in the system. All three spectra have been shown in the Figure 3 to highlight the changes observed in the pigment dispersions. Titanium dioxide characteristic peaks include Ti-O bonds which are obtained at 539.97 cm^{-1} and Ti-O-Ti stretching vibrations received at 1457.92 cm^{-1}. Shifts in peak intensity and additional peaks were obtained in the dispersions, mainly due to the incorporation of the surfactants [18].

The additional peaks are obtained at 1037.52 and 1353.78 cm^{-1}, which align to C-O stretching and C-H bending vibrations, respectively, in the PD-T70-Th5 [19]. Other peaks at 3691.09 and 2950.55 cm^{-1} in the PD-T50-K20-Th5 correspond to -OH vibrations. The peak observed at 1037.52 cm^{-1} corresponds to the symmetrical Al-OH bending. The addition of kaolin as the functional filler in PD-T50-K20-Th5 caused these peaks to emerge, containing alumina and water over its surface [20].

3.1.3. Field emission scanning electron microscopy (FE-SEM)

Morphological analysis showed homogeneously distributed, uniformly sized particles of titanium dioxide nanoparticles in PD-T70-Th5. In contrast, heterogeneous dispersion of titanium dioxide nanoparticles over the surface of alumina (calcined kaolin) can be found in the case of PD-T50-K20-Th5 [21]. Higher-resolution micrographs of both dispersions showed roughness on the particles, which is associated with uniform and strong adhesion of surfactants over the surface of the particles. These chemicals increase surface energy, stabilizing the particles to reduce interaction with other particles and prevent agglomeration [22]. The same was confirmed in the particle size analysis of the samples. The former particles are essentially spherical to disc-shaped, while the latter ones appear to have an elliptical instinct in shape. Furthermore, the difference in the titanium dioxide dosage is also reflected in SEM images as the higher intensity of particles can be found in PD-T70-Th5 with no reporting of alumina base [23]. On the other hand, relatively lesser particles of titanium dioxide are seen in the case of PD-T50-K20-Th5, uniformly dispersed over alumina support.
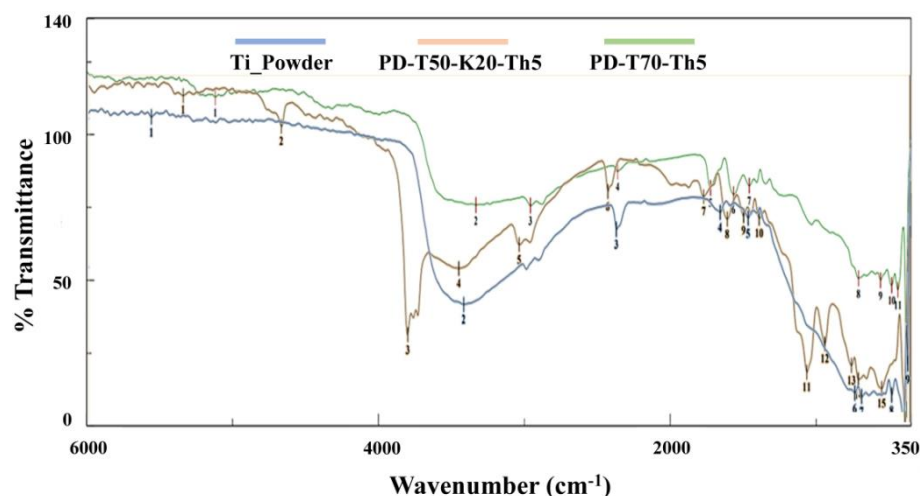

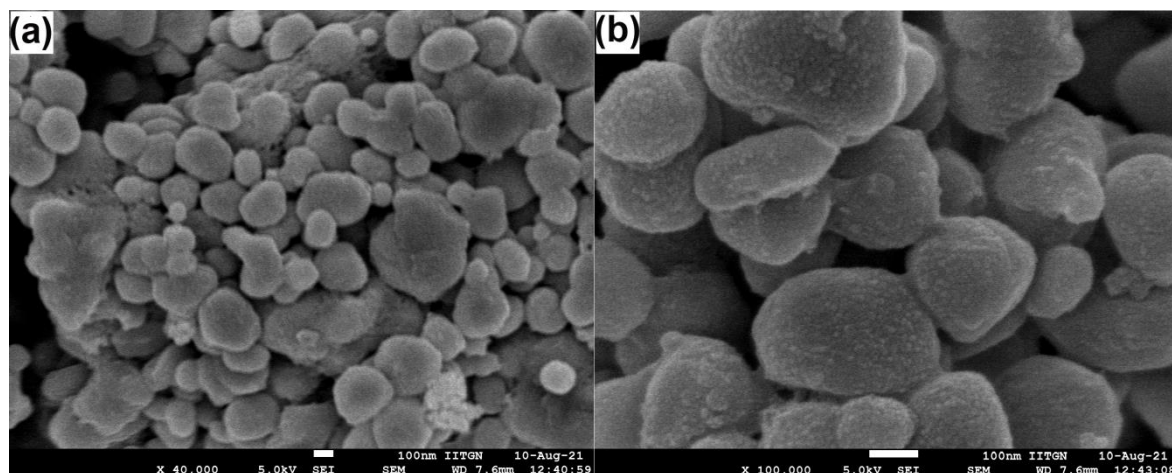**Figure 3:** FT-IR spectra of Titanium Powder, PD-T70-Th5 & PD-T50-K20-Th5.

Figure 4: SEM Micrograph of PD-T70-Th5 (zooming of and 40,000x (a) and 100,000x (b)).
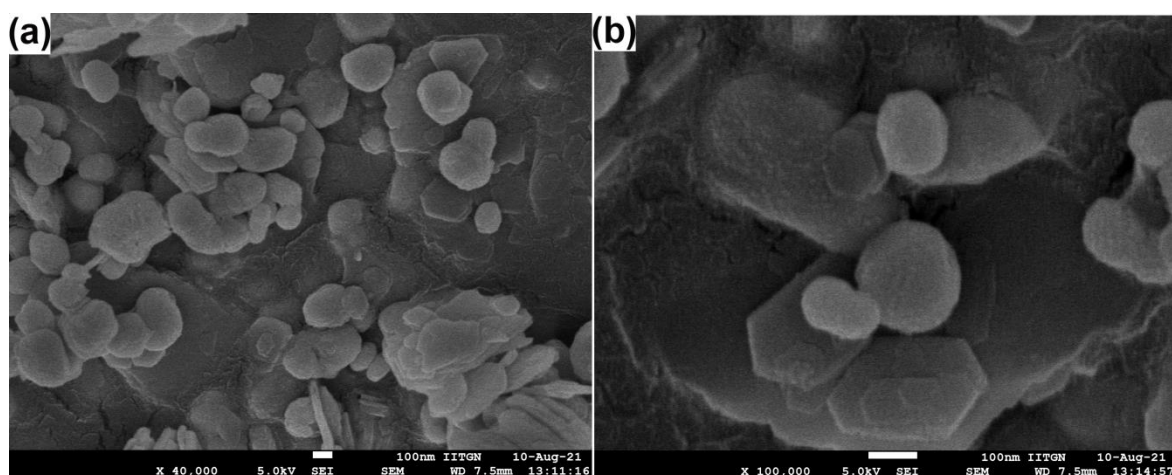

Figure 5: SEM Micrograph of PD-T50-K20-Th5 (zooming of and 40,000x (a) and 100,000x (b)).

3.1.4. X-Ray diffraction

Moisture dried PD-T70-Th5, and PD-T50-K20-Th5 samples were subjected to powder x-ray diffraction to understand the structure of particles through phase analysis to evaluate the material's crystal structure. It was conducted using a Bruker D8 advance diffractometer. Peak analysis was carried out for the 2θ range of 10-90 degrees with an increment of 0.01987 degrees using Cu-K_α incident radiation of 0.154 nm wavelength.

Similar patterns were found in the case of diffraction patterns of both PD-T70-Th5 and PD-T50-K20-Th5 dispersions. In the case of PD-T70-Th5, higher intensity peaks were obtained at a slight angle shift, which is associated with higher titanium dioxide concentrations. The nature of the diffraction pattern, in terms of sharp intensity peaks and minimal noise, corresponds to the highly crystalline structure of the material [24]. The crystallographic planes present in the sample are: 110 (27.77, 27.43), 101 (36.39, 36.05), 111 (41.56, 41.22), 210 (44.36, 44.04), 211 (54.61, 54.30), 220(56.92, 56.60) and 301(69.26, 69.02) for PD-T70-Th5 and PD-T50-K20-Th5 respectively at the mentioned 2θ angle in brackets [25]. Crystallographic sizes of the planes are being calculated using Debye-Scherrer Equation, and values are mentioned below in Table 3.

The average crystallite size for PD-T70-Th5 and PD-T50-K20-Th5 is 52.97 and 55.43 nm, respectively (Figure 6). It was calculated by measuring the intensity of peaks along with their crystallographic plane size. In the case of PD-T70-Th5, crystallite size follows the particle size analysis as the d_{50} size is 49.9 nm. Thus, it can be inferred that these particles are essentially mono-crystalline. The same thing is also confirmed by the SEM micrograph [26]. For PD-T50-K20-Th5, average particle size, d_{50} (183.4 nm) is over 3 times its average crystalline size, which indicates its poly-crystalline nature although it is not of short-range order. It indicates agglomeration of certain (order of units to tenths) nanoparticles over alumina, which can also be seen in the SEM micrograph [27].

Table 3: Crystallite size table for different crystallographic planes of PD-T70-Th5 and PD-T50-K20-Th5.

Sr. No.	Diffraction Angle-2θ (deg.)		Crystallographic Plane (hkl)	Crystallite Size (nm)	
	PD-T70-Th5	PD-T50-K20-Th5		PD-T70-Th5	PD-T50-K20-Th5
1	27.770	27.410	110	47.990	54.349
2	36.390	36.050	101	46.316	46.267
3	41.560	41.220	111	47.059	47.009
4	44.360	44.040	210	38.877	37.146
5	54.610	54.300	211	63.664	68.468
6	56.920	56.600	220	64.344	69.191
7	69.280	68.980	301	68.763	53.385
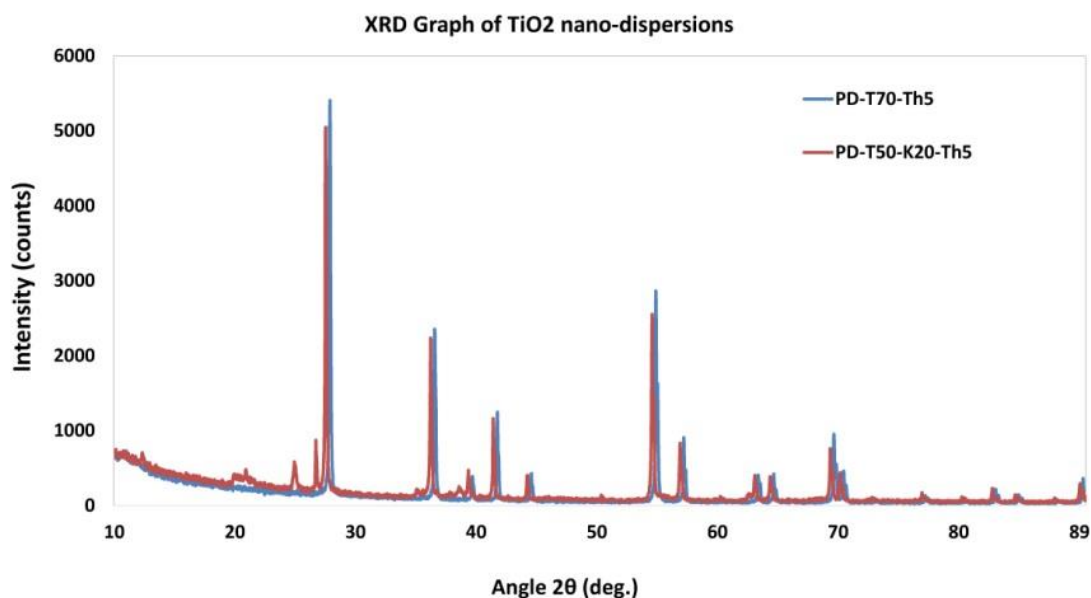
Figure 6: XRD pattern of PD-T70-Th5 and PD-T50-K20-Th5 dispersions.

3.2. Physiochemical properties of pigment dispersions

The physiochemical properties of the pigment dispersions were measured to prepare a basic dataset of it to determine its suitability, performance, and guideline dosage in the wide range of waterborne coatings. Determination of physicochemical properties was carried out using standard ASTM guidelines using compliance devices/equipment in the standard testing conditions to measure data. The physiochemical properties of the dispersions, namely PD-T70-Th5 and PD-T50-K20-Th5 have been mentioned below in the Table 4.

3.3. Effect of process variables on the properties of nano-dispersions

The impact of grinding on the particle size of the pigment and thickener composition on the product's viscosity has been studied to optimize the synthesis process. Grinding time is associated with reducing the particle size of the pigment, which improves dispersion. Also, thickener composition (hydroxyethylcellulose) improves the rheological properties of the product.

3.3.1. Grinding effect on the pigment particle-size

The pre-dispersed rheological solution blended with additives and the titanium dioxide powder pigment and extender is subjected to grinding in the bead mill to decrease its particle size. After a predetermined period, the dispersion samples were taken and subjected to PSA analysis to study the rate of reduction of the particle size to establish a grinding time for desired output particle size. Particle size, d_{50}, has been considered for the analysis. The size-reduction curve has been established on a pigment particle-size basis.

Both grinding processes started with the average particle size of powder pigment, which turns out to be 1121.3 nm. The difference in the rate of particle size reduction, as indicated by Figure 7, was found mainly due to differences in the composition of pigment & extender. For both the pigment dispersions, much of the total decline was found in stage-1. A significant drop in particle size reduction beyond 200 nm was observed in stage-2. [28]. Reduction in the particle size of PD-T50-K20-Th5 was found to be lesser than PD-T70-Th5 since it contained calcined kaolin with the pigment-to-extender ratio of 5:2, and adhesion of pigment particles over its' surface resulted in negligible particle size reduction beyond 200 nm. The output particle size in PD-T70-Th5 and PD-T50-K20-Th5 at the end of stage-1 were 226.2 and 336.2 nm, respectively, which ultimately reduced to 49.9 and relatively lesser 183.4 nm respectively at the end of the two-staged grinding process, combinedly carried out for 7 hours [29]. Particle size reduction was observed at a significantly lower rate in stage-2 since pigment particles were approaching ultrafine particle size. It was nearly stalled after 90 minutes in the case of PD-T50-K20-Th5, which appears to be the optimum time for processing when extenders are to be processed into the synthesis of dispersions. Moreover, polydispersity index (PI) after 7 hours of processing was found to be 0.285 and 0.355 respectively in PD-T70-Th5 and PD-T50-K20-Th5, which relates to the narrower size distribution in the former as compared to the latter [30].

Table 4: Physiochemical properties of PD-T70-Th5 and PD-T50-K20-Th5 dispersions.

| Sr. No.	Property	Standard	Value / Characteristic		Unit
			PD-T70-Th5	**PD-T50-K20-Th5**	
1	Colour Index (TiO$_2$)	ASTM D1394-76	Pigment White Six (CI 77891)		-
2	Physical Appearance	-	Milky White Paste		-
3	Density	ASTM D1475-13	1.937 ± 0.100	1.952 ± 0.100	gm/cm^3
4	Solids Content	ASTM D2369-20	75.00 ± 02.00	78.00 ± 03.00	% w/w
5	Viscosity (Brookfield)	ASTM D2196-20	$37,000 \pm 2.000$	$38,500 \pm 2,000$	mPa.s
6	pH (10% w/w aq. sol^n)	ASTM E70-19	8.75 ± 0.50	8.25 ± 0.50	-
7	Adhesion (Cross-hatch)	ASTM D3359	5A	5A	-
8	Compatibility	-	Miscible with water and emulsions used in water-based coatings		-

Particle-Size Reduction Curve
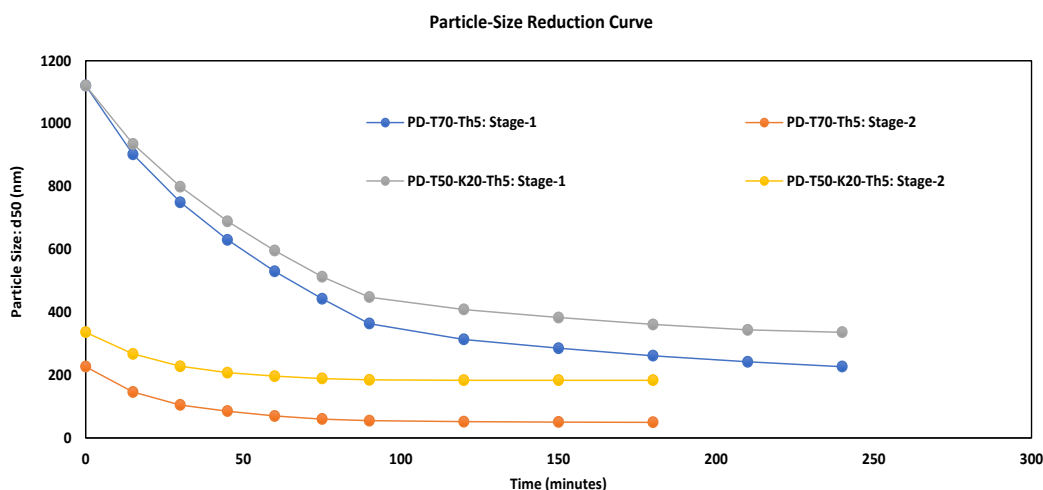
Figure 7: Particle-Size Reduction Curve of PD-T70-Th5 & PD-T50-K20-Th5.

3.3.2. Effect of rheological variables on dispersion applications

The rheological analysis is one of the critical factors that determines and regulates the coatings' flow properties. The flow properties of coatings having different compositions of hydroxyethyl cellulose (rheology modifier) were measured by the viscosity of the dispersions to evaluate their flow properties [31]. Dilution of synthesized distributions with a different fraction(s) of distilled water was conducted to measure viscosity drop in the system to establish rheological data for commonly adopted pigment dosage in the coatings industry. Moreover, analysis with styrene-acrylic copolymer emulsion was also conducted to investigate dispersion interaction with the binder. The analysis was performed using a fungi lab viscolead advance viscometer [32].

3.3.2.1. Effect of water-dilution on dispersion viscosity

All synthesized pigment dispersions were subjected to dilution with water in the dispersion to water mass fraction range of 00.10-00.40, which is the common range for the pigment to water ratio for most of the practical industrial applications [33]. Figure-8 represents the nature of viscosity drop for different dispersions for the predefined range of dilution. Analysis was conducted at room temperature (28 °C)

using the L1 spindle at 100 RPM as the input parameters.

From the Figure 8, it can be noted that the composition of pigment and extender affected the nature of the drop since the dispersions with kaolin content initially exhibited higher drops than one without kaolin. Higher thickener compositions only increased systems viscosity, and no significant effect on viscosity drop was found. For all dispersions, viscosity drops were found to be nearly linear below 0.2 weight fraction (% w/w) [34]. Thus, concentrations of the dispersions affect the solution viscosity at higher weight fractions which is desirable for general waterborne primers and topcoats.

3.3.2.2. Effect of combined water-emulsion system on viscosity

Copolymer Emulsion, which acts as a binder for coatings, and water, which is the system base, are the two main ingredients of most waterborne coating systems in terms of their dosage. Thus, viscosity measurements of this system would closely exhibit viscosities identical to that of the final coatings. Emulsion-water solutions of different compositions (70:30, 60:40 and 50:50 %w/w) were prepared initially, after which different compositions of pigment to solution were prepared ranging from 10-40 % of pigment dispersion in the emulsion-water solution [35].

For the 70:30 emulsion to water ratio, which is generally adopted in high-performance UV-stable exterior coatings, viscosity curves were found to increase nature along with dosage increment of the pigment dispersions (Figure 9). The viscosity of the stock emulsion solution was measured to be 15.5 CST at 28 °C (L2 spindle at 100 RPM). The nature of the graph, as shown in Figure 9, demonstrates step increment at the mass fractions of 0.15 and 0.30, respectively, with the former being very smooth and the latter being relatively steep. The difference in the drop of viscosities of PD-T70-Th5 (70:30 solution) and PD-T50-K20-Th5 (70:30 solution) showed narrowing of the gap with the decrement of the dispersion dosage [36]. Moreover, two-step increments were reported at weight fractions of 0.15 and 0.30, with the latter being higher in magnitude than the former. The increment is related to the interaction of hydroxyethyl cellulose present in the dispersions with the emulsion-water system, which associates with the higher system stability at those concentrations.
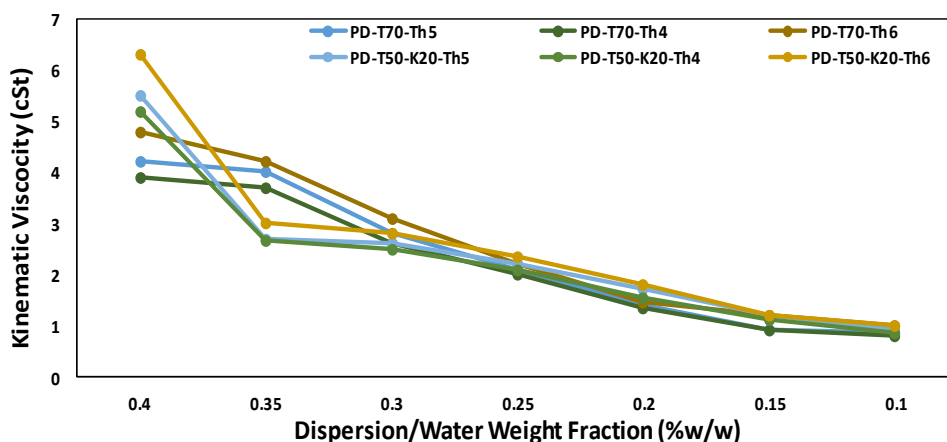
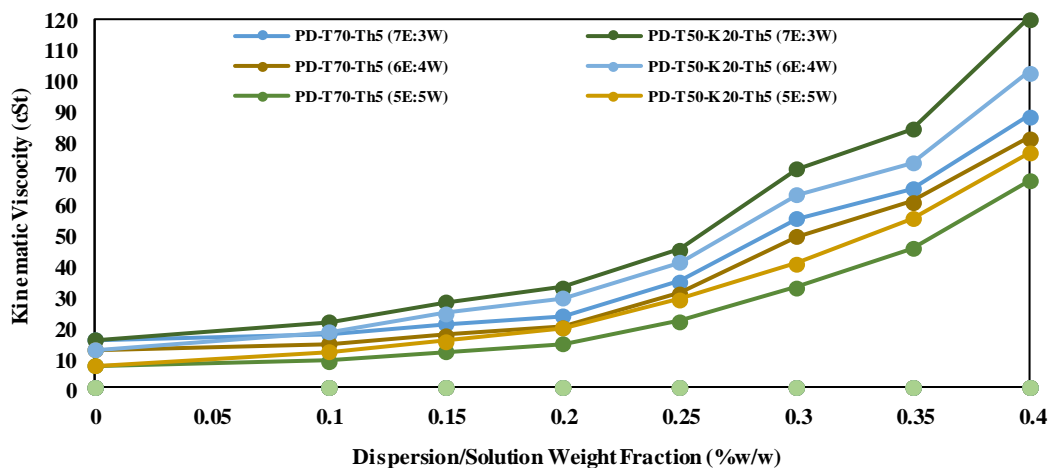**Figure 8:** Dilution viscosity drop curve for pigment dispersions.

Figure 9: Viscosity plots for synthesized dispersions in emulsion-water system.

Similar patterns were observed with minor changes were observed in the case of 60:40 and 50:50 percentages of emulsion to water solutions. Due to increased water concentration, the step-increment intensity at 0.15 and 0.30 was reduced in the 60:40 solution system. Moreover, viscosity increment in 50:50 solution was found to be nearly linear in terms of rate of increment with no reporting of step-increment concentration within measuring range. One common observation from viscosity analysis indicated a relatively higher viscosity increment for dispersions with the kaolin composition than those without it. Thus, viscosity analysis in the emulsion-water solution system provides an effective dataset for synthesizing waterborne coatings with custom requirements of rheological properties suitable to the specific application.

4. Conclusion

The present study shows a novel approach towards synthesizing ultrafine titanium dioxide (rutile) based nano-crystalline dispersions for its application as a pigment in waterborne coatings. Three staged, scalable technology has been adopted to synthesize nanoparticles to establish their use in coatings industries. Characterization techniques confirmed the presence of nanoparticles in dispersed form. Cumulative operations of particle size analysis exhibited stable nanoparticles, which are highly non-interacting, to prevent agglomeration. Moreover, SEM

micrographs also demonstrated the homogeneous distribution of the particles with a uniform coating of surfactants over the particles. It associates higher surface energy and stability, which aligns with the results obtained in particle size analysis regarding the stability and interaction of particles. Powdered XRD analysis confirmed the presence of nano-crystals, with PD-T70-Th5 being essentially mono-crystalline and PD-T50-K20-Th5 having an order of 3-4 crystallographic planes in its structure. As for commercial considerations of its potential application, these dispersions contain 70 % and 50 % of rutile grade titanium dioxide, which is why they are likely to be cost-effective solutions and substitution to powder pigments, due to its virtue of improved properties by addition of different surfactants.

5. References

1. Titanium Dioxide Market Size, Share & Trends Analysis Report By Application (Paints & Coatings, Plastics, Pulp & Paper, Cosmetics), By Region (APAC, North America, Europe), And Segment Forecasts, 2021 – 2028 (Report ID: 978-1-68038-705-6), *Grand View Research* (2021).

2. S. Middlemas, Z. Z. Fang, P. Fan, A new method for production of titanium dioxide pigment. *Hydrometal.,* 131(2013), 107-113.

3. M. J. Gázquez, J. P. Bolivar, F. García-Tenorio García-Balmaseda, F. Vaca, A review of the production cycle of titanium dioxide pigment, *Sci. Res.*, 5(2014), 441-458.

4. V. González-Rodríguez, D. L. Zapata-Tello, J. Vallejo-Montesinos, R. Z. Nunez, J.A. Gonzalez-Calderon, E. Perez, Improving titanium dioxide dispersion in water through surface functionalization by a dicarboxylic acid, *J. Disp. Sci. Tech.*, 27(2018), 33-45.

5. F. Raoufi, Z. Ranjbar, S. Rategar, E. Nowak, B. Nazari, Wettability study of superHydrophobic silica aerogel powders. *Prog. Color Colorants Coat.*, 13(2020), 75-83.

6. B. C. Lane, Additives in water-borne coatings, Royal Society of Chemistry, Cambridge (UK), 2003, Issue No. 290.

7. J. S. Taurozzi, V. A. Hackley, M. R. Wiesner, A standardised approach for the dispersion of titanium dioxide nanoparticles in biological media. *Nanotoxi.,* 7.4(2013), 389-401.

8. P. Dumitru, I. Jitaru, The impact of rheology modifiers on the viscosity of decorative water based paint upon tinting, *UPB Sci. Bull., Series B,* 73.1 (2011), 27-36.

9. M. Takeda, E. Tanabe, T. Iwaki, A. Yakubi, K. Okuyama, Preparation of nanocomposite microspheres containing high concentration of TiO₂ nanoparticles via bead mill dispersion in organic solvent, *Chem. Lett.,* 38.5(2009), 448-449.

10. I. M. Joni, A. Purwanto, F. Iskandar, K. Okuyama, Dispersion stability enhancement of titania nanoparticles in organic solvent using a bead mill process, *Ind. Eng. Chem. Res.,* 48.15(2009), 6916-6922.

11. C. Agbo, W. Jakpa, B. Sarkodie, A. Boakye, S. Fu, A review on the mechanism of pigment dispersion, *J. Disp. Sci. Tech.,* 39.6(2018), 874-889.

12. S. Nagose, E. Rose, A. Joshi, Study on wetting and dispersion of the Pigment Yellow 110, *Prog. Org. Coat.,* 133(2019), 55-60.

13. F. Karakaş, B. V. Hassas, K. Ozhan, F. Boylu, M. S. Celik, Calcined kaolin and calcite as a pigment and substitute for TiO2 in water based paints, In *XIV Balkan Mineral Processing Congress, Bosnia Herzegovina,* (2011), 461-464.

14. W. M. Hess, Characterization of dispersions, *Rub. Chem. Tech.,* 64.3(1991), 386-449.

15. H. Choi, W. Lee, J. Lee, H. Chung, W. S. Choi, Ultra-fine grinding of inorganic powders by stirred ball mill: Effect of process parameters on the particle size distribution of ground products and grinding energy efficiency, *Met. Mater. Int.,* 13.4(2007), 353-358.

16. L. F. Hakim, D. M. King, Y. Zhou, C. J. Gump, S. M. George, A. W. Weimer, Nanoparticle coating for advanced optical, mechanical and rheological properties, *Adv. Func. Mater.,* 17.16(2007), 3175-3181.

17. M. Khajeh Aminian, T. Azizi, R. Dehghan, M. Hakimi, Synthesis and Characterization of CoAl₂O₄ Nano Pigments by Polyol Method, *Prog. Color Colorants Coat.,* 10(2017), 231-238.

18. K. Vajda, K. Saszet, E.Z. Kedves, Z. Kasa, V. Danciu, L. Baia, K. Magyari, K. Hernadi, G. Kovacs, Z. Pap, Shape-controlled agglomeration of TiO₂ nanoparticles New insights on polycrystallinity vs. single crystals in photocatalysis, *Cera. Int.,* 42.2(2016), 3077-3087.

19. M. Rashvand, Z. Ranjbar, Cathodic electrodeposion of nano Titania along the epoxy based coating and evaluation of its anticorrosion properties, *Prog. Color Colorants Coat.,* 7.4(2014), 227-235.

20. S.P. Yeap, J. Lim, H.P. Ngang, B.S. Ooi, A.L. Ahmad, Role of particle–particle interaction towards effective interpretation of Z-average and particle size distributions from dynamic light scattering (DLS) analysis, *J. Nano. Nanotech.,* 18.10(2018), 6957-6964.

21. W. Su, J. Zhang, Z. Feng, T. Chen, P. Ying, C. Li, Surface phases of TiO₂ nanoparticles studied by UV Raman spectroscopy and FT-IR spectroscopy, *J. Phy. Chem., C,* 112.20 (2008), 7710-7716.

22. B.A. Abdulmajeed, S. Hamadullah, F. A. Allawi, Deep oxidative desulfurization of model fuels by prepared nano TiO₂ with phosphotungstic acid, *J. Eng.,* 24.11(2018), 41-52.

23. A. Mohammadi, A. Aliakbarzadeh Karimi, H. Fallah Moafi, Adsorption and photocatalytic properties of surface-modified TiO₂ nanoparticles for methyl orange removal from aqueous solutions, *Prog. Color Colorants Coat.,* 9(2016), 249-260.

24. B. Wang, H. Ding, Y. Deng, Characterization of calcined kaolin/TiO₂ composite particle material prepared by mechano-chemical method, *J. Wuhan Uni. Tech. Mater. Sci. Ed.,* 25.5(2010), 765-769.

25. D. G. Yu, J. H. An, Titanium dioxide core/polymer shell hybrid composite particles prepared by two-step dispersion polymerization, *Coll. Surf. A: Physico. Eng. Asp.,* 237.1-3(2004), 87-93.

26. Y. J. Yang, A. V. Kelkar, X. Zhu, G. Bai, H. T. Ng, D. S. Corti, E. I. Frances, Effect of sodium dodecylsulfate monomers and micelles on the stability of aqueous dispersions of titanium dioxide pigment nanoparticles against agglomeration and sedimentation, *J. Coll. Int. Sci.,* 450(2015), 434-445.

27. Z. Ranjbar, S. Ashhari, A. Jannesari, S. Montazeri, Effects of nano silica on the Anticorrosive properties of epoxy coatings, *Prog. Color Colorants Coat.,* 6.2(2013), 119-128.

28. Y. Gu, X. Zhao, Y. Liu, Y. Lv, Preparation and tribological properties of dual-coated TiO₂ nanoparticles as water-based lubricant additives, *J. Nanomat., 2014*(2014), 112569.

29. M. Hosseinnezhad, M. Ghahari, H. Shaki, J. Movahedi, Investigation of DSSCs performance: the effect of 1,8-naphthalimide dyes and Na-doped TiO₂., *Prog. Color Colorants Coat.,* 13(2020), 177-185.

30. T. Theivasanthi, A. Marimuthu, Titanium dioxide (TiO2) nanoparticles XRD analyses: an insight, *arXiv:1307.1091 [physics.chem-ph], Cornell University,* (2013), 1-10.

31. M. A. Ramazanov, F. V. Hajiyeva, A. M. Maharramov, A. B. Ahmadova, U. A. Hasanova, A. M. Rahimli, H. A. Shirinova, Influence of polarization processes on the morphology and photoluminescence properties of PP/TiO₂ polymer nanocomposites, *Acta Phys. Pol. A,* 131.6(2017), 1540.

32. R. M. Omer, E. T. B. Al-Tikrity, R. N. Abed, M. Kadhom, A. H. Jawad, E. Yousif, Electrical conductivity and surface morphology of PVB films doped with different nanoparticles, *Prog. Color Colorants Coat.,* 15(2022), 191-202.

33. M. Anis, M. S. Pandian, M. I. Baig, P. Ramasamy, G. G. Muley, Monocrystal growth and characterization study of α-and γ-polymorph of glycine to explore superior performance of γ-glycine crystal, *Mater. Res. Innov.,* 22.7(2018), 409-414.

34. J. Epp, X-ray diffraction (XRD) techniques for materials characterization, *Materials characterization using nondestructive evaluation (NDE) methods,* Woodhead Publishing, 2016, 81-124.

35. A. Madhi, B. Shirkavand Hadavand, A. Amoozadeh, Thermal conductivity and viscoelastic properties of

UV-curable urethane acrylate reinforced with modified Al_2O_3 nanoparticles, *Prog. Color Colorants Coat.*, 10(2017), 193-204.

36. K. Ohenoja, M. Illikainen, J. Niinimäki, Effect of operational parameters and stress energies on the particle size distribution of TiO_2 pigment in stirred media milling, *Powder Tech.,* 234(2013), 91-96.

37. K. Hrininh, R. Hordeichuk, O. Gubenia, Comparative analysis of equipment and research the superfine grinding process of titanium dioxide and quinacridone red suspensions in the bead mill, *Ukrainian J. Food Sci.,* 6(2018), 82-94.

38. T. Ogi, R. Zulhijah, T. Iwaki, K. Okuyama, Recent progress in nanoparticle dispersion using bead mill, *KONA Powd. Parti. J.,* (2017), 2017004.

39. S. S. Gwebu, H. Chiririwa, The effect of hydroxyl ethyl cellulose (HEC) and hydrophobically–modified alkali soluble emulsions (HASE) on the properties and quality of water based paints, *Int. J. App. Chem.,* 13.1(2017), 1-13.

40. A. H. Nour, Emulsion types, stability mechanisms and rheology: A review, *Inter. J. Innov. Res. Sci. Stud. (IJIRSS),* 1.1(2018).

41. P. Dumitru, I. Jitaru, The impact of rheology modifiers on the viscosity of decorative water based paint upon tinting, *UPB Sci. Bull., Series B,* 73.1(2011).

42. S. Rouhani, M. Hosseinnezhad, S. Nasiri, K. Gharanjig, A. Salem, Z. Ranjbar, Investigation of the effect of rGO/TiO_2 on photovoltaic performance of DSSCs devices, *Prog. Color Colorants Coat.,* 15(2022), 123-131.

43. A. K. Van Dyk, T. Chatterjee, V. V. Ginzburg, A. I. Nakatani, Shear-dependent interactions in hydrophobically modified ethylene oxide urethane (HEUR) based coatings: Mesoscale structure and viscosity, *Macromol.,* 48.6(2015), 1866-1882.

44. J. Clayton, Pigment/dispersant interactions in water-based coatings, *Surf. Coat. Int.,* 80.9(1997), 414-420.

45. R. A. Bhavsar, K. M. Nehete. Rheological approach to select most suitable associative thickener for water-based polymer dispersions and paints, *J. Coat. Tech. Res.,* 16.4(2019), 1089-1098.